

---

# APP: Anytime Progressive Pruning

---

**Diganta Misra\***

Mila - Quebec AI Institute, Landskape AI, UdeM

**Bharat Runwal\***

Landskape AI, IIT-Delhi

**Tianlong Chen**  
VITA, UT-Austin

**Zhangyang Wang**  
VITA, UT-Austin

**Irina Rish**  
Mila - Quebec AI Institute, UdeM

{diganta, bharat}@landskape.ai

## Abstract

With the latest advances in deep learning, there has been a lot of focus on the online learning paradigm due to its relevance in practical settings. Although many methods have been investigated for optimal learning settings in scenarios where the data stream is continuous over time, sparse networks training in such settings have often been overlooked. In this paper, we explore the problem of training a neural network with a target sparsity in a particular case of online learning: the anytime learning at macroscale paradigm (ALMA). We propose a novel way of progressive pruning, referred to as *Anytime Progressive Pruning* (APP); the proposed approach significantly outperforms the baseline dense and Anytime OSP models across multiple architectures and datasets under short, moderate, and long-sequence training. Our method, for example, shows an improvement in accuracy of  $\approx 7\%$  and a reduction in the generalization gap by  $\approx 22\%$ , while being  $\approx 1/3$  rd the size of the dense baseline model in few-shot restricted imagenet training. We further observe interesting nonmonotonic transitions in the generalization gap in the high number of megabatches-based ALMA. The code and experiment dashboards can be accessed at <https://github.com/landskape-ai/Progressive-Pruning> and <https://wandb.ai/landskape/APP>, respectively.

## 1 Introduction

Supervised learning has been one of the most well-studied learning frameworks for deep neural networks, where the learner is provided with a dataset  $\mathcal{D}_{x,y}$  of samples( $x$ ) and corresponding labels( $y$ ); and the learner is expected to predict the label  $y$  by learning on  $x$  usually by estimating  $p(y|x)$ . In an offline learning environment Ben-David et al. [1997], the learner has access to the complete dataset  $\mathcal{D}_{x,y}$ , while in a standard online learning setting Sahoo et al. [2017], Bottou et al. [1998] the data arrive in a stream over time, assuming that the rate at which samples arrive is the same as that of the learner’s processing time to learn from them. There are several fine-grained types of learning from a stream of data, including, but not limited to, continuous learning Van de Ven and Tolias [2019], Thrun [1995], Ring [1998], active online learning Baram et al. [2004], Settles [2009], and anytime learning Grefenstette and Ramsey [1992], Ramsey and Grefenstette [1994]. In an anytime learning framework, the learner has to have good performance at any point in time, while gradually improving its performance over time upon observing new data that subsequently arrive.

Anytime Learning at Macroscale(ALMA) Caccia et al. [2021] recently introduced a new subparadigm of learning inspired by anytime learning and transfer learning Pan and Yang [2009]. In ALMA, the

---

\*Equal contribution

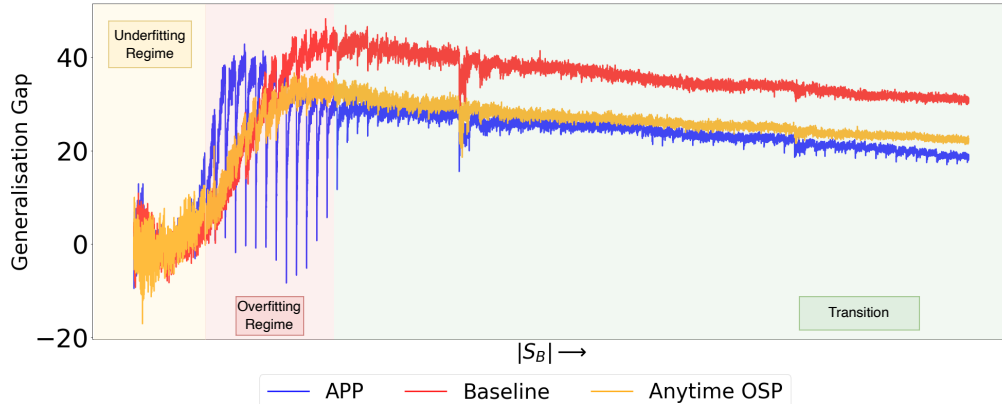


Figure 1: **Non-Monotonic Transition:** Generalization gap as a function of the number of megabatches ( $|S_B| = 100$ ) in the long-sequence ALMA setting with full replay for ResNet-50 backbone on the CIFAR-10 dataset. We observe that APP consistently demonstrates the *lower* generalization gap compared to anytime OSP and baseline models. The curve for APP showcases high oscillation in the critical regime where the model starts overfitting, which can be attributed to the regularization effect induced by the pruning at the start of each megabatch.

time it takes for the model to be trained on a set of samples called a megabatch is significantly shorter than the interval between the arrival of two consecutive megabatch. Thus, ALMA studies the optimal waiting time that corresponds to the mega-batch size to ensure that the model is a good anytime learner. Caccia et al. Caccia et al. [2021] abstractly define a learner trained in an ALMA setting as: “... a learner that i) produces high accuracy, ii) can make non-trivial predictions at any point in time, while iii) limits its computational and memory resources”

In this work, we are interested in exploring the training of sparse(pruned) neural networks in the ALMA setting. Pruning Blalock et al. [2020], Luo et al. [2017], Wang et al. [2021] of overparameterized deep neural networks has been studied for a long time. Pruning deep neural networks leads to a reduction in inference time and memory footprint. Pruning has gained prominence since the inception of the lottery ticket hypothesis (LTH) Frankle and Carbin [2018], Frankle et al. [2019a,b], Malach et al. [2020], which demonstrated the existence of subnetworks (lottery tickets) within a dense network, which, when trained from random initialization in the same setting, will match or outperform the dense network. Although early pruning work focused exclusively on pruning weights after pretraining the dense model for a certain number of iterations, extensive research has recently been conducted on pruning the model at initialization, that is, finding the lottery ticket from a dense model at the start without pretraining the dense model Lee et al. [2018], Wang et al. [2020a]. However, few studies Chen et al. [2020] have investigated the training of sparse(pruned) neural networks in online settings. Thus, our objective is to answer the following question:

“Given a dense neural network and a target sparsity, what should be the optimal way of pruning the model in ALMA setting?”

In summary, our contributions can be summarized by the following four points.

- \* We provide the first comprehensive study into pruning of deep neural networks in an ALMA setting. Specifically, we conclude through extensive empirical evaluation that progressive pruning consistently outperforms different baselines. We define the baselines used for comparison in Section 3.
- \* We therefore propose a novel approach of progressively pruning dense neural networks in the ALMA paradigm, which we term **Anytime Progressive Pruning**(APP).
- \* We further investigate the training dynamics of APP as compared to the baselines in ALMA setting with varied number of megabatches using CIFAR-10, CIFAR-100 and Restricted ImageNet datasets, and, observe non-monotonic transition graphs in their generalization gap during training.

- \* Furthermore, we do conclusive ablation studies to investigate the different types of pruners that are compatible with APP and one-shot pruning (OSP) models, along with studying the effect of replay. We conclude that APP outperforms OSP when all  $t - 1$  megabatches are replayed while training on the  $t$ -th megabatch; however, OSP models outperform APP models when no replay buffer is used.

In the following section, we provide concrete insights into the motivation of the problem statement that we investigate in this paper, derived from the foundations of active learning and practical data acquisition (collection, annotation, and labeling).

## 1.1 Motivation

A well-accepted statement in deep learning states “*Collection of unlabeled data is relatively easy, however, labeling is costly and difficult.*” This is arguably true because labeling or annotating data requires a human in the loop with extensive domain knowledge, which induces an additional cost in addition to the cost in the form of computing power required to train the learner. Active learning Baram et al. [2004], Settles [2009], Olsson [2009], Liu et al. [2021], Dimitrakakis and Savu-Krohn [2008] is a well-studied domain in machine learning that particularly investigates training of data-efficient models under cost constraints. Specifically, given a learner and a set of unlabeled data, an active learning algorithm will select particular samples to label via an oracle, under a predetermined cost budget, to maximize performance. This framework is not only limited to the labeling of unlabeled data, but can also be extended to label correction or reannotation of noisy labeled data. In Bernhardt et al. [2021], the authors study optimal reannotation strategies under resource constraints to achieve a maximal performance gain, which they call active label cleaning. The authors of Settles et al. [2008] study the annotation times and costs of different data sets in the real world domain. They report the variation in cost and time required to label different sets of unlabeled data.

Reiterating from the previous section, we are interested in understanding and finding the optimal strategy for training sparse neural networks given a target sparsity in the ALMA setting. Often, in industrial and practical scenarios, there exists a fixed initial period for the collection of data, which is subsequently labeled by an oracle. For this problem statement, we assume knowledge of the total number of samples that the learner will observe, which allows us to predetermine the required number of megabatches. We assume that the complete stream of data is already acquired but unlabeled and that the individual megabatches received in the stream by the learner are labeled over time by an oracle. This allows us to optimally select the wait time (megabatch size) and study the interesting properties of the training dynamics of models trained on these megabatches in an ALMA setting.

## 2 Related Work

### 2.1 Pruning

Pruning LeCun et al. [1990], Han et al. [2015a] as one of the effective model compression techniques is widely explored in the field of efficient machine learning. It trims down the parameter redundancy in modern over-parameterized deep neural networks, aiming at substantial resource savings and unimpaired performance. Depending on the granularity of the removed network components, classical pruning methods can be categorized into unstructured Han et al. [2015a], LeCun et al. [1990], Han et al. [2015b] and structural pruning Liu et al. [2017], Zhou et al. [2016], where the former removes parameters irregularly and the latter discards substructures such as convolution filters or layers. In addition to the above post-training pruning, it can also be flexibly applied before network training, such as SNIP Lee et al. [2019], GraSP Wang et al. [2020b] and SynFlow Tanaka et al. [2020] or during training Zhang et al. [2018], He et al. [2017]. The key factor in these methods is the estimation of the importance of pruning targets, which can be learned Zhang et al. [2018], He et al. [2017] using data-driven methods or approximated by some heuristics of the training dynamics, including weight magnitude Han et al. [2015a], gradient Molchanov et al. [2019], hessian LeCun et al. [1990].

Recent closely related work Chen et al. [2021] defines pruning in sequential learning as a dynamical system and proposes two effective lifelong pruning algorithms to identify high-quality subnets, leading to superior trade-offs between efficiency and lifelong learning performance. Furthermore, Golkar et al. [2019] prunes neurons with low activity and Sokar et al. [2020] compresses the sparse connections of each task during training to overcome the problem of forgetting.

## 2.2 Lifelong Learning

Lifelong learning Ring et al. [1994], Thrun [1995], Ring [1998], Thrun [1998] has gained increasing attention from the deep learning community. Numerous algorithms developed can be roughly divided into two categories: (i) one group of methods Wang et al. [2017], Rosenfeld and Tsotsos [2018], Rusu et al. [2016], Aljundi et al. [2017], Rebuffi et al. [2018], Mallya et al. [2018] accommodate newly added tasks/classes by accordingly growing the network capacity. However, it usually suffers from the explosive model size, which is proportional to the number of classes. (ii) the other group of approaches mainly takes advantage of advances in transfer learning Kemker and Kanan [2017], Belouadah and Popescu [2018], where the quality of pre-trained embeddings plays an essential role. In particular, Li and Hoiem [2017], Castro et al. [2018], Javed and Shafait [2018], Rebuffi et al. [2017], Belouadah and Popescu [2019, 2020] adopt replay methods with some stored past training data to alleviate catastrophic forgetting in sequential learning. Furthermore, more follow-ups use imbalance learning techniques He and Garcia [2009], Buda et al. [2018] or knowledge distillation regularizations Li and Hoiem [2017], Castro et al. [2018], He et al. [2018], Javed and Shafait [2018], Rebuffi et al. [2017], Belouadah and Popescu [2019, 2020] to further improve its performance on all learned tasks.

## 2.3 Revisiting ALMA

In this section, we revisit the ALMA learning framework as conceptualized in Caccia et al. [2021]. Based on the reasoning provided in the original paper, we explicitly focus on classification problems. In ALMA, the model  $f_\theta$  is provided with a stream of  $S_B$  of  $|S_B|$  consecutive batches of samples under the assumption that there exists an underlying data distribution  $\mathcal{D}_{x,y}$  with input  $x \in \mathbb{R}^d$  and target labels  $y \in \{1, \dots, C\}$ . Each megabatch  $\mathcal{M}_t$  consists of  $N \gg 0$  i.i.d. samples randomly drawn from  $\mathcal{D}_{x,y}$ , for  $t \in \{1, \dots, S_B\}$ . Therefore, the stream  $S_B$  is the ordered sequence  $S_B = \{\mathcal{M}_1, \dots, \mathcal{M}_{|S_B|}\}$  where  $|S_B|$  represents the total number of megabatches in the stream. Thus, the model  $f_\theta : \mathbb{R}^d \rightarrow \{1, \dots, C\}$  is trained by processing a *mini-batch* of  $n \ll N$  samples at a specified time of each mega-batch  $\mathcal{M}_t$  and iterating multiple times over each mega-batch before having access to the next mega-batch. In ALMA, it is assumed that the rate at which megabatches arrive is slower than the training time of the model on each megabatch, and, therefore, the model can iterate over the megabatches at its disposal based on its discretion to maximize performance. ALMA can be considered a special case of continual learning (CL) or lifelong learning Ring et al. [1994], Thrun [1995], Ring [1998], Thrun [1998], whose data distribution across batches (or tasks) is considered stationary. Compared to CL, the difficulty in ALMA is fewer data in each learning stage, while the challenge in CL is the dynamic data distributions across different learning stages. Meanwhile, ALMA is also loosely relevant to online learning Saad [1998] with the key difference that ALMA receives large batch data sequentially rather than in a stream.

In ALMA, one of the main aims was to study the effect of variation in waiting time, which directly corresponds to the size of each megabatch, i.e. how long one should wait to collect samples for a particular megabatch. Furthermore, the authors conducted a conclusive study using different baselines, two of them being (a) ensemble and (b) dynamic growing. In both cases, the complexity of the model parameters was gradually increased to allocate sufficient capacity to accommodate the newly arrived megabatches. However, in this paper, we investigate the effect of progressively decreasing the parametric complexity of the model through pruning and subsequently training a sparse neural network in an ALMA setting.

## 3 Anytime Progressive Pruning

In this section, we formally introduce our proposed method *Anytime Progressive Pruning*(APP). As demonstrated in Figure 2, given a randomly initialized dense neural network  $f_\theta$ , a target sparsity  $0.8^\tau \times 100\%$ , and the first megabatch  $\mathcal{M}_1 \in S_B$  containing  $|\mathcal{M}_1|$  samples, we use 20% random samples in  $\mathcal{M}_1$  denoted as  $\pi_1$  and pass them to SNIP Lee et al. [2018] together with  $f_\theta$  and prune the model to  $0.8^{\delta_1} \times 100\%$  in one iteration at initialization. After pruning, we take the pruned network  $f_\theta^1$  and train it on  $\mathcal{M}_1$  for  $k$  epochs. For the next sequence  $\mathcal{M}_2$ , we first concatenate the entire previous megabatch  $\mathcal{M}_1$  into the current megabatch  $\mathcal{M}_2$  that gives  $\mathcal{M}_1 \cup \mathcal{M}_2$  and then take the best performing checkpoint of the trained model on  $\mathcal{M}_1 - f_{\theta_1}^1$  and again use 20% random samples in

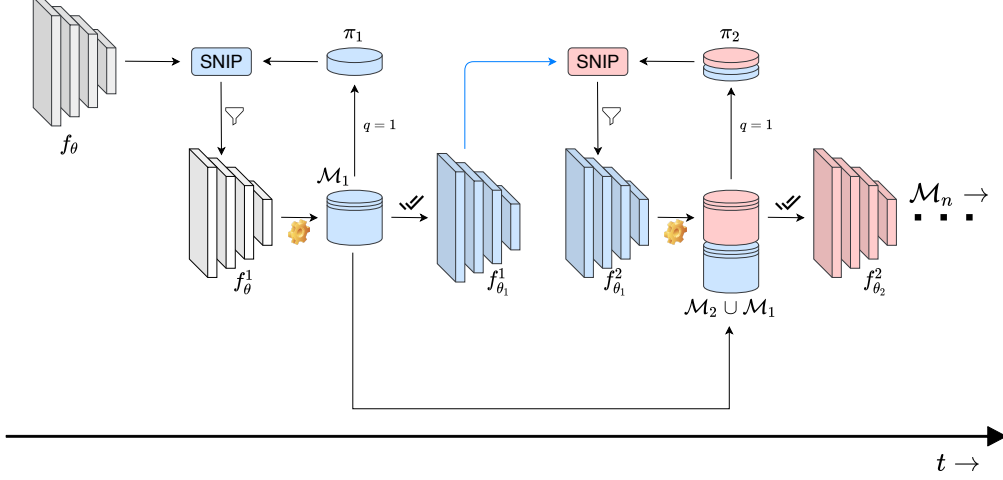


Figure 2: Overview of **Anytime Progressive Pruning** (APP) using full replay with a given randomly initialized dense model  $f_\theta$  and  $|S_B|$  total megabatches.

$\mathcal{M}_1 \cup \mathcal{M}_2$  denoted as  $\pi_2$  and pass them to SNIP to prune  $f_{\theta_1}^1$  by further  $0.8^{\delta_2} \times 100\%$  and use the resultant model  $f_{\theta_1}^2$  to train it on  $\mathcal{M}_1 \cup \mathcal{M}_2$ .

---

**Algorithm 1** Training APP in the ALMA setting

---

**Require:**  $f_\theta^{t=0}, \tau, \text{replay}, S_B \iff \{\mathcal{M}_1, \dots, \mathcal{M}_{|S_B|}\}$

- 1:  $t \leftarrow 1$
- 2:  $\delta \leftarrow \{start = 1, end = \tau, steps = |S_B|\}$  ▷ Pruning states at each megabatches
- 3: **while**  $t \leq |S_B|$  **do** ▷ For each megabatch based training
- 4:   SNIP set( $\pi_t$ )  $\leftarrow \emptyset$
- 5:   **if** replay **then**
- 6:      $\mathcal{M}_t \leftarrow \bigcup_{i=1}^t \mathcal{M}_i$
- 7:   **else**
- 8:      $\mathcal{M}_t \leftarrow \mathcal{M}_t$
- 9:   **end if**
- 10:   pruning state  $\leftarrow 0.8^{\delta_t}$  ▷ Target Sparsity ( $\times 100\%$ ) at each megabatch
- 11:   SNIP set  $\leftarrow \pi_t \subset \mathcal{M}_t \mid \frac{|\pi_t|}{|\mathcal{M}_t|} = 0.2$
- 12:    $f_\theta^t \leftarrow \text{SNIP}(f_\theta^{t-1}, \text{SNIP set}, \text{pruning state})$
- 13:    $f_\theta^t.train(\mathcal{M}_t)$  ▷ Fine-tune or retrain from scratch
- 14: **end while**

---

Thus, for each megabatch  $\mathcal{M}_t \in S_B$ , we construct the replay inclusive megabatch  $\mathcal{M}_t$  by taking the union of all previous megabatches along with the current megabatch and then create a small sample set  $\pi_t$  of size  $0.2 * |\mathcal{M}_t|$  to be used to prune the model to  $0.8^{\delta_t} \times 100\%$  sparsity. Here,  $\delta_t$  is obtained from a predetermined list  $\delta$  of uniformly spaced values that denote the target sparsity levels for each megabatch in the stream  $S_B$ . After pruning the model, we train it on the  $\mathcal{M}_t$  megabatch and evaluate it on a holdout test set.

**Note:**

- \* The operator  $|\cdot|$  denotes the size of a given set throughout this paper.
- \*  $|\theta|$  denotes the number of trainable parameters in millions.
- \* By default, APP always uses full replay buffer.
- \* For all experiments, the scope of pruning was maintained to be *Global*.
- \*  $0.8^\tau \times 100\%$  represents the fraction of weights left from the initial dense model post pruning and not the fraction of weights pruned, which would be denoted as  $(1 - 0.8^\tau) \times 100\%$ .

To evaluate APP, we use primarily 2 baselines:

1. **Baseline:** This denotes the standard model (e.g., convolution neural network or transformer) at full parametric capacity trained and fine-tuned on all megabatches in the stream  $S_B$  using stochastic gradient descent in an ALMA setting.
2. **Anytime OSP:** This denotes one-shot pruning (OSP) to the target sparsity  $0.8^\tau \times 100\%$  at the initialization of  $f_\theta$  and then subsequently training on all mega-batches in the stream  $S_B$  in an ALMA setting. Thus, anytime OSP models have the lowest parametric complexity since the start of training on the first megabatch in the stream  $S_B$ . We use the same pruner of choice (SNIP) by default for both APP and Anytime OSP. Similarly to APP, we prune the model at initialization using a small randomly selected subset  $\pi_1$  of the first megabatch  $\mathcal{M}_1$  of size  $0.2 * |\mathcal{M}_1|$ .

We use the following metric along with the test accuracy and the generalization gap to evaluate the methods specified above.

1. **Cumulative Error Rate (CER):** This can be defined by the following equation:

$$CER = \sum_{t=1}^{S_B} \sum_{j=1}^{|T_{x,y}|} \mathbb{1}(\mathcal{F}_t(x_j) \neq y_j) \tag{1}$$

Here,  $T_{x,y}$  represents the held-out test set used for evaluation,  $\mathcal{F}_t$  represents the trained model at  $t$ -th megabatch and  $\mathcal{F}_t(x_j)$  represents the prediction on the  $j$ -th index sample of the test set  $T_{x,y}$  compared to the true label for that sample  $y_j$ . CER provides strong insights into whether the learner is a good anytime learner, as it is expected to minimize CER at each megabatch training in the stream  $S_B$ .

We follow the standard definition of the generalization gap as the difference between the training and the validation accuracy. This gives a notion of whether the model is over- or under-fitting.

## 4 Experiments

In this section, we provide in-depth details on the experimental setup, the learning algorithms, and the data sets used in our empirical evaluation. We further discuss the training dynamics observed under the variation of  $|S_B|$  and supplement our results with a visualization of the training curves.

### Datasets

We empirically evaluated APP, Anytime OSP, and Baseline models on three different data sets: (a) CIFAR-10 (C-10) Krizhevsky et al. [2009] (b) CIFAR-100 (C-100) Krizhevsky et al. [2009] and (c) Restricted Imagenet (balanced) Engstrom et al. [2019], Tsipras et al. [2018]. Both C-10 and C-100 consist of 50,000 training images and 10,000 test images, each of size 32 x 32, divided into 10 and 100 classes, respectively. Restricted ImageNet (balanced) is a subset of the original ImageNet data set Russakovsky et al. [2015] consisting of 89517 training images and 3450 test images, each of 224 x 224 size divided into 14 classes consisting of five subclasses each. For our experimental analysis, we conduct benchmarks on both the 224 x 224 size version and additionally a 32 x 32 size version where we down-sample each image using bilinear interpolation.

Taking into account the three datasets mentioned above, we construct benchmarks for the evaluation of APP as follows: (1) we randomly partition the data set into  $|S_B|$  megabatches with an equal number of samples in each megabatch, (2) for each megabatch  $\mathcal{M}_T \in S_B$ , we partition it into a train set comprising 90% samples in  $\mathcal{M}_t$  and a validation set of the remaining 10% samples in  $\mathcal{M}_t$ , (3) from each megabatch we randomly extract 20% of the training data to build the set  $|\pi_t|$  used for pruning via SNIP, and (4) we create the training pipeline where the learner is pruned using  $\pi_t$  and subsequently trained on the megabatch at the current state for  $k$  iterations. We keep a separate held-out test set, which is not seen by the learner during training, but is used to evaluate the model’s performance after completion of training on each megabatch.

## Models

For our experiments, we use mainly four standard vision classifiers: (a) ResNet-18 He et al. [2016], (b) ResNet-50 He et al. [2016], (c) VGG-16 (with Batch Normalization) Simonyan and Zisserman [2014], and (d) Wide ResNet-50 Zagoruyko and Komodakis [2016]. We specifically picked these models because of their popularity in standard computer vision tasks and the extensiveness of the studies conducted on these models for various learning paradigms. However, for long-sequence-based ALMA (high number of megabatches) and restricted ImageNet experiments, we only use ResNet-50 as the model of choice. In addition, all models were trained from scratch, and no pre-training was used.

## Hyperparameters and learning setup

Here, we describe in detail the experimental setups that were used for the reported results and discuss the difference in performance between APP, Anytime OSP, and baseline models in different scenarios. As mentioned above, for the experimental evaluation, we focus primarily on the task of image classification using the models defined in Subsection 4. For all experiments excluding a single VGG-16 + BN ablation study, we used a fixed target sparsity  $\tau = 4.5$ , which means, for all APP and Anytime OSP-based results, the model was pruned to have only 36.63% remaining weights compared to the initial dense baseline network, which corresponds to  $\approx \frac{1}{3}$ rd model capacity post pruning. We hardcoded  $\tau$  to 4.5, as we observe an inconsistency in performance for APP models at higher levels of sparsity, as reported in Table 2.

We use the following two learning setups for our empirical validation.

1. **SGD with multi-step decay at  $\mathcal{M}_1$  only:** All results reported in Table 2 were trained using Stochastic Gradient Descent (SGD) with a momentum of 0.9 and an initial learning rate of 0.1, along with multistep decay of the learning rate by  $\gamma = 0.1$  at the 91<sup>st</sup> and 136<sup>th</sup> epoch only for the first megabatch ( $\mathcal{M}_1$ ). For all subsequent megabatches  $\mathcal{M}_2 \dots \mathcal{M}_t$ , a constant learning rate of 0.001 was maintained. Each megabatch was trained for 182 epochs except the  $|S_B| = 25$  run reported in Table 5.
2. **SGD with cyclic multi-step decay at every  $\mathcal{M}_t$ :** All results in Table 4 (excluding the results highlighted in light yellow), 6 and 7 were trained using SGD with the same initial parameters as described above. However, after completion of the training on each megabatch  $\mathcal{M}_t$ , the learning rate was reset to its initial state of 0.1.

While we tested various pruning algorithms for the APP and Anytime OSP models such as SNIP Lee et al. [2018], magnitude pruning, random pruning, IMP Frankle and Carbin [2018], and GraSP Wang et al. [2020b], we use SNIP by default because we observe higher stability and training performance when coupled with APP. We use the default parameters for the pruning algorithms specified above and provide additional details in the supplementary section.

## 4.1 Results

### 4.1.1 Ablation study with CIFAR-10 ALMA

We conducted initial experiments to validate the design choice used in the default version of APP for all experiments conducted in this research. We used the following different versions of APP for the experiment:

**Note:** All experiments were carried out using a ResNet-50 backbone on CIFAR-10 using a fixed target sparsity of  $\tau = 4.5$  with a total of 8 megabatches consisting of each 6250 samples. Furthermore, all reported results were obtained with a cyclic learning rate policy only for the first mega-batch  $\mathcal{M}_1$ , and subsequent mega-batches had a fixed learning rate.

1. **APP Default:** This is the default version of APP adopted in all the experiments in this manuscript. The exact algorithm is defined in Section 3.
2. **APP + WD (1e-4):** This version of APP follows the same algorithm as that of the default, however, adds a weight decay of 1e-4 to the weight updates at each iteration.

3. **APP Final:** In this version of APP, we apply the pruning at the end of each megabatch training, contrary to the default version where we prune the model at the beginning of each megabatch.
4. **APP Warmup:** In this version of APP, we apply the pruning after a few warm-up epochs (20) at each megabatch, contrary to the default version where we prune the model at the beginning of each megabatch.
5. **APP no replay SNIP:** In this version of APP, we construct the subset  $\pi_t$  used by SNIP for pruning only from the current megabatch  $\mathcal{M}_t$  and do not include any samples from the megabatch in the replay buffer  $\mathcal{M}_1 \dots \mathcal{M}_{t-1}$ .

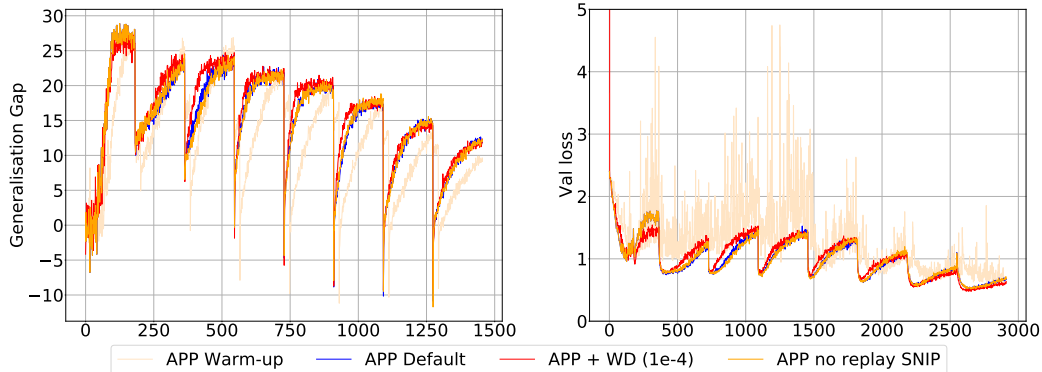


Figure 3: From left to right: (a) Generalization gap for various versions of APP. (b) Validation loss for various versions of APP.

As shown in Table 1, APP + WD (1e-4) obtains the highest test accuracy, while APP warm-up has the lowest generalization gap compared to the default version of APP. However, we do not use weight decay by default due to inconsistent results across various models and settings. Although APP warm-up provides a drop of the generalization gap by a margin of 2.64% compared to APP default, we do not use it as default due to the reduction in test accuracy by a margin of 1.8% compared to APP default, and additionally the training of the same was extremely unstable, as shown in Fig. 3. Furthermore, we note that the training collapses when used with APP Final version, while for the case of APP no-replay SNIP, we observe a drop in both the test accuracy and the generalization gap compared to APP default.

Table 1: Ablation study for the choice of APP design.

Method	Test Accuracy( $\uparrow$ )	Generalization Gap( $\downarrow$ )
APP Default	84.65%	11.816%
APP + WD (1e-4)	<b>85.6%</b> (+0.95 %)	12.336%(+0.52 %)
APP Final	37.2%	65.333% <sup>†</sup>
APP Warm-up	82.85%(-1.8 %)	<b>9.176%</b> (-2.64 %)
APP no replay SNIP	83.35%(-1.3 %)	11.976%(+0.16 %)

#### 4.1.2 Analysis of short sequence ALMA ( $|S_B| = 8$ )

We start by analyzing the results reported in Table 2. All experiments were carried out using full replay ( $\mathcal{M}_t \leftarrow \bigcup_{i=1}^t \mathcal{M}_i$ ) for a total of 8 megabatches ( $|S_B| = 8$ ) with each megabatch containing  $|\mathcal{M}_t| = 6250$  samples.

For ResNet-18 trained on C-10, we observe that APP (SNIP) decreases the test accuracy by 0.68% and decreases the generalization gap by 6.718% compared to the baseline model. Although the Anytime OSP (SNIP) model outperforms APP (SNIP) by a small margin of 0.21%, the former has a significantly higher generalization gap compared to the latter by 6.867%. For C-100, we observed



a strong improvement in APP (SNIP) in test accuracy compared to the baseline by a margin of 3.85%, while the generalization gap was drastically reduced by 30.187%. Similar improvements were observed for the CER metric as reported in the table and the improvements were consistent when using magnitude-based pruning for APP.

For ResNet-50, we observed an even greater performance improvement for APP (SNIP) compared to the baseline and Anytime OSP models in all metrics: test accuracy, CER, and generalization gap. For example, in C-10, the use of APP (SNIP) improved the test accuracy by 5.46%, decreased the CER by 1278, and decreased the generalization gap by 7.393% while the use of Anytime OSP (SNIP) resulted in a decrease in the test accuracy by 3.1%, an increase in the CER by 4268, and an increase in the generalization gap by 3.11% compared to the baseline model. We observe for C-10 that the use of APP (SNIP) with a small weight decay of  $1e-4$  results in an improvement in the test accuracy by 0.95% compared to the version without weight decay. However, we did not conduct extensive studies to validate the improvement caused by weight decay, as it is beyond the scope of our experimental evaluation. We observe a similar improvement in performance from baseline when coupled with weight decay.

The improvement in performance is also observed in Wide ResNet-50, where for C-10, APP (SNIP) outperforms the baseline model in test accuracy by 11.04%, reduces CER by 6095 and reduces the generalization gap by 12.007%. However, for VGG-16 with batch normalization, we did not observe a significant improvement in performance from the baseline model compared to its Anytime OSP counterpart.

For all experiments, we observed strong results for APP when used with SNIP and magnitude-based pruning. In our observations, while Anytime OSP is stable and compatible with other pruning methods such as random pruning and GraSP, APP causes a significant loss in performance when used with the same. This is the reason why we chose to fix SNIP as the pruner of choice for APP. We observe that APP with random pruning and GraSP continues to perform at par with its SNIP and magnitude-based pruning counterparts for the initial megabatches, but with increasing sparsity, causes a detrimental effect on the accuracy curves, as shown in Fig. 6a. Furthermore, for VGG-16 with batch normalization, we conducted an experiment to study the effect of high sparsity for the training of C-10 where we set  $\tau = 13$ , which implies that the model had  $\approx 5.5\%$  remaining parameters after pruning. However, we observed that APP causes a significant reduction in performance at this high level of sparsity.

Table 2: Results on ALMA of C-10 and C-100. † denotes unstable training. WD denotes a weight decay of  $1e-4$  being used during training.

Backbone	Method	Pruner	$\theta(\downarrow)$	Test Accuracy( $\uparrow$ )		CER( $\downarrow$ )		Generalization Gap( $\downarrow$ )	
				CIFAR-10	CIFAR-100	CIFAR-10	CIFAR-100	CIFAR-10	CIFAR-100
ResNet-18	Baseline	-	11.51 M	86.37%	54.44%	14618	42535	13.64%	47.08%
	Baseline (WD)	-	11.51 M	<b>88.75%</b> (+2.38%)	55.2(+0.76%)	11840(-2778)	42269(-266)	11.0%(-2.64%)	46.553%(-0.527%)
	Anytime OSP	SNIP Lee et al. [2018]	4.09 M	<b>85.9%</b> (-0.47%)	54.09%(-0.35%)	14276(-342)	42785(+250)	13.789%(+0.149%)	47.753%(+0.673%)
	APP	SNIP Lee et al. [2018]	4.09 M	85.69%(-0.68%)	<b>58.29%</b> (+3.85%)	<b>13476</b> (-1142)	<b>42442</b> (-93)	<b>6.922%</b> (-6.718%)	<b>16.893%</b> (-30.187%)
	Anytime OSP	Magnitude	4.09 M	<b>86.2%</b> (+0.17%)	54.06(-0.38%)	<b>14486</b> (132)	42090(-445)	13.611%(-0.029%)	47.94%(+0.86%)
	APP	Magnitude	4.09 M	85.58%(-0.79%)	<b>58.07%</b> (+3.63%)	16109(+1491)	<b>41966</b> (-569)	<b>10.76%</b> (-2.88%)	<b>22.676%</b> (-24.404%)
ResNet-50	Baseline	-	23.5 M	79.19%	44.56%	19221	49471	19.20%	56.63%
	Baseline (WD)	-	23.5 M	<b>83.15%</b> (+3.96%)	44.66%(+0.06%)	18143(-1078)	49879(+408)	16.991%(-2.18%)	57.233%(+0.602%)
	Anytime OSP	SNIP Lee et al. [2018]	8.6 M	76.09%(-3.1%)	41.07%(-3.53%)	23489(+4268)	51829(+2588)	22.32%(+3.11%)	59.853%(+3.222%)
	APP	SNIP Lee et al. [2018]	8.6 M	<b>84.65%</b> (+5.46%)	<b>52.01%</b> (+7.41%)	17943(-1278)	<b>48164</b> (-1077)	<b>11.816%</b> (-7.393%)	<b>23.002%</b> (-33.629%)
	APP (WD)	SNIP Lee et al. [2018]	8.6 M	<b>85.6%</b> (+6.41%)	-	-	-	12.336%(-6.873%)	-
	Anytime OSP	Magnitude	8.6 M	78%(-1.19%)	45.06%(+0.46%)	21365(+2144)	48859(-382)	19.83%(+0.62%)	56.356%(-0.275%)
	APP	Magnitude	8.6 M	<b>83.63%</b> (+4.44%)	<b>51.94%</b> (+7.34%)	19078(-143)	<b>48032</b> (-1209)	<b>6.913%</b> (-12.296%)	<b>22.871%</b> (-33.76%)
	Anytime OSP	IMP	8.6 M	78.99%(-0.2%)	-	-	-	20.227%(+1.018%)	-
	APP	IMP	8.6 M	<b>83.63%</b> (+4.44%)	-	-	-	<b>6.913%</b> (-12.296%)	-
	Anytime OSP	Random	8.6 M	<b>75.59%</b> (-3.6%)	<b>47.07%</b> (+2.47%)	23745(+4524)	<b>47646</b> (-1595)	23.333%(+4.124%)	<b>54.787%</b> (-1.844%)
	APP	Random	8.6 M	62.63%(-16.56%)	1.67%†	24390(+5169)	55163(+5922)	7.373%†	35.004%†
	Anytime OSP	GraSP Wang et al. [2020b]	8.6 M	<b>83.26%</b> (+4.07%)	<b>46.06%</b> (+1.46%)	17442(-1779)	<b>49244</b> (+3)	<b>16.862%</b> (-2.347%)	<b>55.52%</b> (-1.111%)
	APP	GraSP Wang et al. [2020b]	8.6 M	10.0%†	2.04%†	33415(+14194)	56254(+7013)	0.1556%†	35.582%†
	Wide ResNet-50-2	Baseline	-	68.9 M	74.45%	47.42%	25299	47273	24.79%
Baseline (WD)		-	68.9 M	84.28%(+9.83%)	51.31%(+3.89%)	17782(-7517)	45232(-2041)	14.578%(-10.218%)	50.718%(-3.278%)
Anytime OSP		SNIP Lee et al. [2018]	25.2 M	79.33%(+4.88%)	<b>49.22%</b> (+1.8%)	19815(-5484)	<b>46052</b> (-1221)	19.724%(-5.072%)	53.096%(-0.9%)
APP		SNIP Lee et al. [2018]	25.2 M	<b>85.49%</b> (+11.04%)	48.18%(+0.76%)	<b>19204</b> (-6095)	48579(+1306)	<b>12.789%</b> (-12.007%)	<b>38.64%</b> (-15.356%)
Anytime OSP		Magnitude	25.2 M	76.05%(+1.6%)	49.48%(+2.06%)	23900(-1399)	<b>46174</b> (-1099)	22.409%(-2.387%)	52.538%(-1.458%)
APP		Magnitude	25.2 M	<b>85.28%</b> (+10.83%)	<b>54.42%</b> (+7.0%)	<b>18675</b> (-6624)	46697(-576)	<b>12.291%</b> (-12.545%)	<b>43.096%</b> (-10.9%)
Anytime OSP		Random	25.2 M	<b>81.43%</b> (+6.98%)	<b>44.5%</b> (-2.92%)	<b>18567</b> (-6732)	49195(+1922)	<b>18.396%</b> (-6.4%)	<b>57.393%</b> (+3.397%)
APP		Random	25.2 M	53.94%(-20.51%)	39.45%(-7.97%)	25673(-374)	<b>48929</b> (+1656)	67.84%†	17.324%†
Anytime OSP		GraSP Wang et al. [2020b]	25.2 M	<b>81.49%</b> (+7.04%)	<b>48.54%</b> (+1.12%)	<b>18452</b> (-6847)	-	<b>17.311%</b> (-7.485%)	53.902%(-0.094%)
APP		GraSP Wang et al. [2020b]	25.2 M	10.78%†	26.27(-21.15%)	29621(+4322)	55129(+7856)	63.273%†	41.589%†
VGG-16-BN	Baseline	-	138.42 M	87.37%	53.52%	12412	42410	11.747%	48.329%
	Baseline (WD)	-	138.42 M	<b>88.29%</b> (+0.72%)	54.85%(+1.33%)	<b>11828</b> (-584)	41122(-1288)	11.451%(-0.296%)	45.767%(-2.568%)
	Anytime OSP	SNIP Lee et al. [2018]	50.6 M	<b>87.59%</b> (+0.02%)	52.51%(-1.01%)	<b>12374</b> (-38)	42575(+165)	12.24%(+0.493%)	47.811%(-0.518%)
	APP	SNIP Lee et al. [2018]	50.6 M	86.76%(-0.81%)	<b>55.31%</b> (+1.79%)	12782(-6370)	<b>41285</b> (-1125)	<b>10.113%</b> (-1.634%)	<b>30.942%</b> (-17.387%)
	Anytime OSP	SNIP Lee et al. [2018]	7.61 M	<b>86.75%</b> (-0.82%)	-	<b>13141</b> (+729)	-	11.067%(-0.68%)	-
	APP	SNIP Lee et al. [2018]	7.61 M	59.5%(-28.07%)	-	20073(+7661)	-	-0.9733%†	-
	Anytime OSP	Magnitude	50.6 M	<b>87.33%</b> (-0.24%)	53.27%(-0.25%)	<b>12551</b> (+139)	<b>42306</b> (-104)	12.476%(+0.729%)	47.996%(-0.333%)
	APP	Magnitude	50.6 M	86.04%(-1.57%)	<b>54.59%</b> (+1.07%)	12943(+531)	42310(-100)	9.862%(-1.885%)	<b>22.369%</b> (-25.96%)
	Anytime OSP	Random	50.6 M	<b>87.49%</b> (-0.08%)	<b>53.82%</b> (+0.3%)	<b>12539</b> (+127)	<b>41739</b> (-671)	<b>12.533%</b> (+0.786%)	<b>46.609%</b> (-1.66%)
	APP	Random	50.6 M	68.56%(-19.01%)	53.01%(-18.51%)	16760(+4348)	46427(+4017)	3.258%†	42.362%†
Anytime OSP	GraSP Wang et al. [2020b]	50.6 M	<b>87.04%</b> (-0.53%)	<b>54.55%</b> (+1.03%)	<b>12945</b> (+533)	<b>41449</b> (-961)	13.476%(+1.729%)	<b>47.189%</b> (-1.14%)	
APP	GraSP Wang et al. [2020b]	50.6 M	14.57%†	26.27%†	24131(+11719)	48888(+6478)	56.624%†	41.589%†	

Table 3: Results on anytime learning of CIFAR-10 and CIFAR-100 using 8 mega-batches with 6250 samples per mega-batch with replay. All APP and Anytime OSP experiments used Snip Lee et al. [2018] as the pruner of choice. All experiments also used an SGD + cyclic multistep decay LR at every  $\mathcal{M}_t$ .

Backbone	Method	$ \theta (\downarrow)$	Test Accuracy( $\uparrow$ )		CER( $\downarrow$ )		Generalization Gap( $\downarrow$ )	
			CIFAR-10	CIFAR-100	CIFAR-10	CIFAR-100	CIFAR-10	CIFAR-100
ResNet-18	Baseline	11.51 M	<b>91.43%</b>	60.39%	10545	38771	<b>8.098%</b>	41.033%
-	Anytime OSP	4.09 M	90.56%(-0.87 %)	60.44%(+0.05 %)	11255 (+710)	38755 (-16)	8.778%(+0.68 %)	40.567%(-0.472 %)
-	APP	4.09 M	90.06%(-1.37 %)	<b>63.61%</b> (+3.22 %)	<b>10419</b> (-126)	<b>37048</b> (-1723)	8.442%(+0.344 %)	<b>26.922%</b> (-14.111 %)
ResNet-50	Baseline	23.5 M	85.7%	46.91%	16821	49486	14.289%	54.878%
-	Anytime OSP	8.6 M	88.61%(+2.91 %)	53.76%(+6.85 %)	14209 (-2612)	45092 (-4394)	11.336%(-2.953 %)	49.182%(-5.696 %)
-	APP	8.6 M	<b>90.89%</b> (+5.19 %)	<b>64.88%</b> (+17.97 %)	<b>12294</b> (-4527)	<b>39559</b> (-9927)	<b>9.24%</b> (-5.049 %)	<b>34.387%</b> (-20.491 %)
Wide ResNet-50-2	Baseline	68.9 M	89.65%	52.73%	13471	44866	10.398%	49.931%
-	Anytime OSP	25.2 M	87.5%(-2.15 %)	48.05%(-4.68 %)	15717 (+2246)	48978 (+4112)	12.109%(+1.711 %)	53.64%(+3.709 %)
-	APP	25.2 M	<b>92.02%</b> (+2.37 %)	<b>66.24%</b> (+13.51 %)	<b>12808</b> (-663)	<b>40327</b> (-4539)	<b>7.976%</b> (-2.422 %)	<b>34.791%</b> (-15.14 %)
VGG-16-BN	Baseline	138.42 M	<b>91.53%</b>	59.06%	<b>9950</b>	38615	9.318%	42.667%
-	Anytime OSP	50.6 M	90.63%(-0.9 %)	57.98%(-1.08 %)	10236 (+286)	39024 (+409)	9.187%(-0.131 %)	43.102%(+0.435 %)
-	APP	50.6 M	89.82%(-1.71 %)	<b>62.51%</b> (+3.45 %)	10171 (+221)	<b>36831</b> (-1784)	<b>8.967%</b> (-0.351 %)	<b>33.293%</b> (-9.374 %)

Compared to the results reported in Table 2, we observe in Table 3 that using the cyclic learning rate policy at each megabatch  $\mathcal{M}_t$  significantly improves performance for the three models, the baseline, Anytime OSP, and APP. For example, for ResNet-50, we note an improvement in test accuracy for the baseline model by a margin of 6.51% compared to the baseline model trained with the cyclic learning rate policy only for the first megabatch  $\mathcal{M}_1$  as reported in Table 2. APP consistently outperforms the baseline and anytime OSP models for each experiment conducted on CIFAR-100 with a significant drop in the generalization gap observed for the four backbones used.

Table 4: Results on ALMA of C-10 and C-100 without replay using SGD with cyclic multistep decay at every  $\mathcal{M}_t$ . Rows highlighted in light yellow represent runs done with SGD with multistep decay at  $\mathcal{M}_1$  only.

Backbone	Method	Pruner	$ \theta (\downarrow)$	Test Accuracy( $\uparrow$ )		CER( $\downarrow$ )		Generalization Gap( $\downarrow$ )	
				CIFAR-10	CIFAR-100	CIFAR-10	CIFAR-100	CIFAR-10	CIFAR-100
ResNet-18	Baseline	-	11.51 M	87.42%	53.4%	<b>12834</b>	<b>41919</b>	13.76%	<b>45.44%</b>
-	Anytime OSP	SNIP Lee et al. [2018]	4.09 M	<b>87.72%</b> (+0.3 %)	<b>54.32%</b> (+0.92 %)	13130 (+296)	41989 (+70)	<b>13.28%</b> (-0.48 %)	47.36%(+1.92 %)
-	APP	SNIP Lee et al. [2018]	4.09 M	80.4%(-7.02 %)	41.59%(-11.81 %)	13939 (+1105)	45885 (+3966)	20.036%(+6.276 %)	56.16%(+10.72 %)
ResNet-50	Baseline	-	23.5 M	80.08%	42.06%	21436	51866	20.64%	58.56%
-	Anytime OSP	SNIP Lee et al. [2018]	8.6 M	<b>83.95%</b> (+3.87 %)	<b>46.18%</b> (+4.12 %)	17521 (-3915)	<b>49083</b> (-2783)	16.942%(-3.698 %)	56.64%(-1.92 %)
-	APP	SNIP Lee et al. [2018]	8.6 M	80.86%(-0.78 %)	<b>36.78%</b> (-5.28 %)	<b>17073</b> (-4363)	51068 (-798)	<b>20.462%</b> (-0.178 %)	<b>64.213%</b> (+5.653 %)
ResNet-50	Baseline (WD)	-	23.5 M	69.95%	41.63%	25744	<b>50303</b>	24.213%	57.76%
-	Baseline (WD)	-	23.5 M	78.05%(+8.1 %)	41.14%(-0.51 %)	19925 (-5819)	52049 (+1746)	23.822%(-0.391 %)	63.769%(+6.009 %)
-	Anytime OSP	SNIP Lee et al. [2018]	8.6 M	<b>71.18%</b> (+1.22 %)	38.5%(-3.15 %)	25452 (-292)	<b>52953</b> (+2650)	25.084%(+0.871 %)	56.836%(-0.924 %)
-	APP	SNIP Lee et al. [2018]	8.6 M	67.69%(-2.26 %)	21.12%(-20.53 %)	<b>23568</b> (-2176)	59042 (+8739)	31.236%(+7.023 %)	52.356%(-5.404 %)
-	Anytime OSP	Magnitude	8.6 M	<b>74.48%</b> (+4.53 %)	<b>41.85%</b> (+0.2 %)	<b>22922</b> (-2822)	<b>50932</b> (+629)	25.689%(+1.559 %)	58.827%(+1.067 %)
-	APP	Magnitude	8.6 M	61.31%(-8.64 %)	20.96%(-20.69 %)	28152 (+2408)	59246 (+8943)	<b>13.351%</b> (-10.862 %)	33.956%(-23.804 %)
-	Anytime OSP	Random	8.6 M	<b>70.66%</b> (+0.71 %)	<b>44.08%</b> (+2.43 %)	<b>25828</b> (+84)	<b>49006</b> (-1297)	25.778%(+1.565 %)	57.618%(-0.142 %)
-	APP	Random	8.6 M	28.01%(-41.94 %)	1% <sup>†</sup>	36044 (+10300)	62683 (+12380)	37.742% <sup>†</sup>	25.813% <sup>†</sup>
-	Anytime OSP	GraSP Wang et al. [2020b]	8.6 M	<b>80.14%</b> (+10.19 %)	<b>41.56%</b> (-0.09 %)	<b>18697</b> (7047)	<b>50867</b> (+564)	<b>19.876%</b> (-4.337 %)	<b>53.564%</b> (-4.196 %)
-	APP	GraSP Wang et al. [2020b]	8.6 M	10.0% <sup>†</sup>	3.51% <sup>†</sup>	41747 (+16003)	62672 (+12369)	40.8% <sup>†</sup>	39.378% <sup>†</sup>
Wide ResNet-50-2	Baseline	-	68.9 M	<b>84.08%</b>	<b>47.17%</b>	<b>17484</b>	<b>47725</b>	<b>16.8%</b>	<b>53.44%</b>
-	Anytime OSP	SNIP Lee et al. [2018]	25.2 M	81.43%(-2.65 %)	42.58%(-4.59 %)	18715 (+1231)	52184 (+4459)	18.382%(+1.582 %)	57.28%(+3.84 %)
-	APP	SNIP Lee et al. [2018]	25.2 M	81.46%(-2.62 %)	35.49%(-11.68 %)	18222 (+738)	51062(-3337)	18.72%(+1.92 %)	64.587%(+11.147 %)
VGG-16-BN	Baseline	-	138.42 M	<b>88.1%</b>	<b>52.24%</b>	<b>11796</b>	<b>41873</b>	15.022%	<b>48%</b>
-	Anytime OSP	SNIP Lee et al. [2018]	50.6 M	88.01%(+0.09 %)	50.63%(-1.61 %)	11874 (+78)	42660 (+787)	<b>13.084%</b> (-1.938 %)	52.16%(+4.16 %)
-	APP	SNIP Lee et al. [2018]	50.6 M	81.74%(-6.36 %)	41.62%(-10.62 %)	13598 (+1802)	44935 (+3062)	19.449%(+4.427 %)	61.991%(+13.991 %)

In Table 4, we conducted experiments to validate the effect of no replay for APP, Anytime OSP, and the baseline models for different backbones. From the experiments, we can conclude with high certainty that APP requires full replay of megabatches to provide a performance improvement. As shown in the table, we see that APP models cause a significant decrease in performance, while Anytime OSP models improve performance compared to their baseline counterparts. We hypothesize that the loss in performance is induced by the model restructuring caused by pruning at the start of each megabatch, which can be attributed to the loss in knowledge transfer while transitioning from one megabatch to the next.

#### 4.1.3 Analysis of moderate and long sequence ALMA ( $|S_B| = 25, 50, 100$ )

For validation on variation of  $|S_B|$ , we conducted experiments using only the ResNet-50 model with full replay and with SNIP as the pruner of choice for both APP and Anytime OSP variants as reported in Table 5. Similarly to short-sequence-based ALMA, we observed a strong improvement in performance while using APP compared to the Anytime OSP and baseline models. In particular, when  $|S_B| = 100$ , where each megabatch has  $|\mathcal{M}_t| = 500$  samples, we report an improvement in CER by 105277 compared to the baseline model, which is equivalent to APP correctly classifying

the test set  $T_{x,y}$  of 10,000 samples 10 times compared to the baseline model throughout the training process on the complete stream  $|S_B|$ . Interestingly, we find that the performance of the baseline has a high variation caused by the change in  $|S_B|$  with a deviation in test accuracy of  $\sigma = 4.345\%$ , while APP is extremely stable and is less sensitive to the change in  $|S_B|$  with a deviation in test accuracy of  $\sigma = 1.743\%$  across  $|S_B|$  values of 8, 25, 50 and 100. We further analyze and investigate the training dynamics observed during training moderate- and long-sequence ALMA, which we discuss in detail in Section 4.2.

Table 5: Results of ALMA training of C-10 models with varying  $|S_B|$ .

Backbone	Method	Pruner	$ \theta (\downarrow)$	$ S_B $	$ \mathcal{M}_t $	Test Accuracy( $\uparrow$ )	CER ( $\downarrow$ )	Generalization Gap( $\downarrow$ )
ResNet-50	Baseline	-	23.5 M	25	2000	<b>82.69%</b>	118876	9.978%
-	Anytime OSP	SNIP Lee et al. [2018]	8.6 M	25	2000	78.86%(-3.83 %)	110698 (-8178)	16.284%(+6.306 %)
-	APP	SNIP Lee et al. [2018]	8.6 M	25	2000	79.73%(-2.96 %)	<b>104435 (-14441)</b>	<b>2.916%(-7.062 %)</b>
ResNet-50	Baseline	-	23.5 M	50	1000	79.13%	193384	20.971%
-	Anytime OSP	SNIP Lee et al. [2018]	8.6 M	50	1000	72.91%(-6.22 %)	202212 (+8828)	26.56%(-2.411 %)
-	APP	SNIP Lee et al. [2018]	8.6 M	50	1000	<b>82.0%(+2.87 %)</b>	<b>163503 (-29881)</b>	<b>14.707%(-6.264 %)</b>
ResNet-50	Baseline	-	23.5 M	100	500	70.87%	396572	28.971%
-	Anytime OSP	SNIP Lee et al. [2018]	8.6 M	100	500	78.51%(+7.64 %)	315349 (-81223)	20.133%(-8.838 %)
-	APP	SNIP Lee et al. [2018]	8.6 M	100	500	<b>82.32%(+11.45 %)</b>	<b>291295 (-105277)</b>	<b>16.502%(-12.469 %)</b>

#### 4.1.4 Few shot experiments on Restricted ImageNet

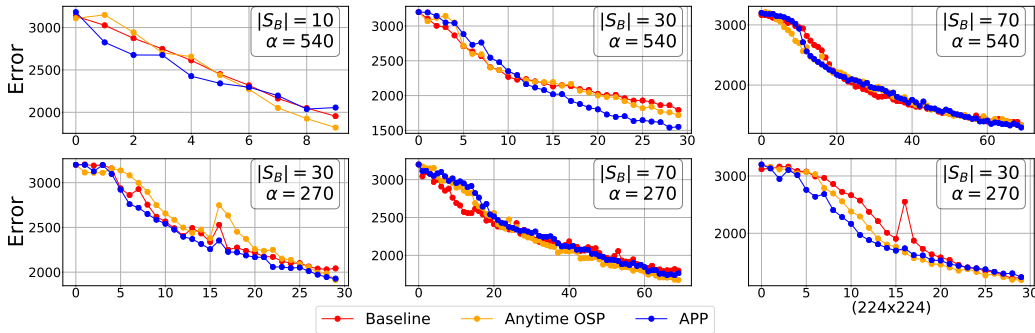


Figure 4: Error rates on the test set of the trained model at each megabatch  $\mathcal{M}_t$  for the restricted Imagenet experiments reported in Table 6.

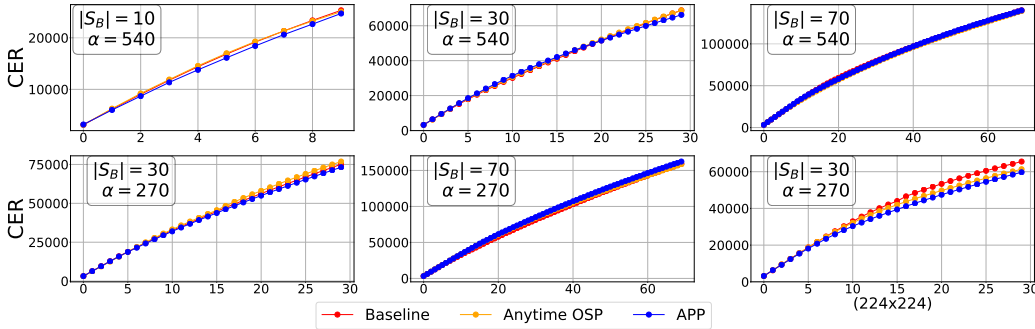


Figure 5: CER of the trained model at each megabatch  $\mathcal{M}_t$  for the restricted Imagenet experiments reported in Table 6.

In this section, we investigate the performance of APP compared to Anytime OSP and the baseline models on Restricted Balanced ImageNet Engstrom et al. [2019], Tsipras et al. [2018] using various few-shot learning settings. We primarily conduct experiments using the following two few-shot settings.

1.  $\alpha = 270$ : For this, we only keep 270 samples per class in the complete dataset, which essentially totals 3780 samples for the complete dataset. We tested this using two different number of megabatches  $|S_B| = 30, 70$  such that each megabatch consists of  $|\mathcal{M}_t| = 126, 54$  samples, respectively. For  $|S_B| = 30$ , we performed experiments on the  $224 \times 224$  and  $32 \times 32$  sizes of the data set. For  $|S_B| = 30$ , we reduce the minibatch size of each megabatch  $\mathcal{M}_t$  to 64 while for  $|S_B| = 70$ , we reduce it to 32.
2.  $\alpha = 540$ : For this, we only keep 540 samples per class in the complete dataset which essentially totals 7560 samples for the complete dataset. We test this using three different number of megabatches  $|S_B| = 10, 30, 70$  such that each megabatch consists of  $|\mathcal{M}_t| = 756, 252, 108$  samples, respectively. For  $|S_B| = 70$ , we reduce the mini-batch size of each megabatch  $\mathcal{M}_t$  to 64.

As reported in Table 6, we observe that APP significantly reduces the generalization gap for each model variant compared to the Anytime OSP and baseline counterparts. Excluding  $\alpha = 270$  with  $|S_B| = 70$  experiment on the  $32 \times 32$  downsampled version of restricted ImageNet, we observe a decrease in CER compared to the baseline model. For example, for  $\alpha = 270$  with  $|S_B| = 30$  on the  $224 \times 224$  version of Restricted Imagenet, we observe that APP reduces the CER by 5846 compared to baseline, which essentially means that APP correctly classified  $\approx 1.5\times$  the test set throughout the training on the full stream  $S_B$ . We also observe strong notable improvements in test accuracy for anytime OSP models in the  $\alpha = 270$  setting, where it records the highest test accuracy in all experiments.

We also visualize and compare the error rate on the test set and CER for each megabatch for APP, Anytime OSP and baseline models in Fig. 4 and Fig. 5 respectively. We observe that while the final CER for APP with  $\alpha = 270$  and  $|S_B| = 70$  is higher than the baseline, this is caused by the higher error rates at the initial megabatches for APP as shown in the fifth subplot (2<sup>nd</sup> row, 2<sup>nd</sup> column) of Fig. 4, while APP at the final megabatches had a lower error than the baseline. In both figures, we observe that APP consistently retains both lower error and CER in almost every megabatch in all settings reported in Table 6.

Table 6: Results on Few-shot ImageNet Restricted ALMA using SGD with cyclic multistep decay at every  $\mathcal{M}_t$ .

Method	Resolution	$ S_B $	$ \mathcal{M}_t $	$\alpha$	Test Accuracy( $\uparrow$ )	CER( $\downarrow$ )	Generalization Gap( $\downarrow$ )
Baseline	32 x 32	10	756	540	43.36%	25328	17.394%
Anytime OSP	-	-	-	-	<b>47.246%</b> (+3.886 %)	24978 (-350)	21.529%(+4.135 %)
APP	-	-	-	-	40.40%(-2.96 %)	<b>24712</b> (-616)	<b>6.963%</b> (-10.431 %)
Baseline	-	30	126	270	40.811%	75128	55.503%
Anytime OSP	-	-	-	-	<b>44.55%</b> (+3.739 %)	76871 (+1743)	48.53%(-6.973 %)
APP	-	-	-	-	44.11%(+3.229 %)	<b>73206</b> (-1922)	<b>34.423%</b> (-21.08 %)
Baseline	-	30	252	540	48.03%	68832	48.733%
Anytime OSP	-	-	-	-	50.23%(+2.2 %)	68765 (-67)	45.288%(-3.445 %)
APP	-	-	-	-	<b>55.04%</b> (+7.01 %)	<b>66239</b> (-2593)	<b>26.388%</b> (-22.345 %)
Baseline	-	70	54	270	47.88%	159204	45.03%
Anytime OSP	-	-	-	-	<b>51.449%</b> (+3.569 %)	<b>158608</b> (-596)	45.357%(+0.327 %)
APP	-	-	-	-	48.898%(+1.018 %)	162360 (+3156)	<b>30.744%</b> (-14.286 %)
Baseline	-	70	108	540	61.391%	140069	34.456%
Anytime OSP	-	-	-	-	61.391%(0%)	<b>139152</b> (-917)	32.979%(-1.477 %)
APP	-	-	-	-	<b>62.492%</b> (+1.101 %)	139963 (-106)	<b>17.5859%</b> (-16.8701 %)
Baseline	224 x 224	30	126	270	64.289%	65525	32.149%
Anytime OSP	-	-	-	-	<b>65.623%</b> (+1.334 %)	61341 (-4184)	33.435%(+1.286 %)
APP	-	-	-	-	64.231%(-0.058 %)	<b>59679</b> (-5846)	<b>29.884%</b> (-2.265 %)

#### 4.1.5 Analysis of training curves and CER for C-10/100

In Fig. 6b and Fig. 6c, we start by analyzing the learning curves, specifically the training accuracy and validation loss curves on C-10 for APP, Anytime OSP, and the baseline models as a function of the total number of training iterations on the entire stream of megabatches  $|S_B|$ . First, in Fig. 6b, we observe a distinct oscillation in the training accuracy curve for APP, which is caused by pruning at the start of training on each new megabatch  $\mathcal{M}_t$ , resulting in a sharp drop in the initial point accuracy.

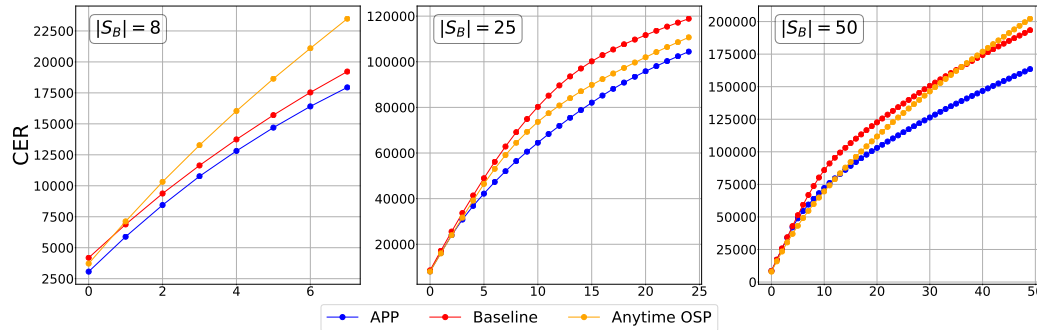
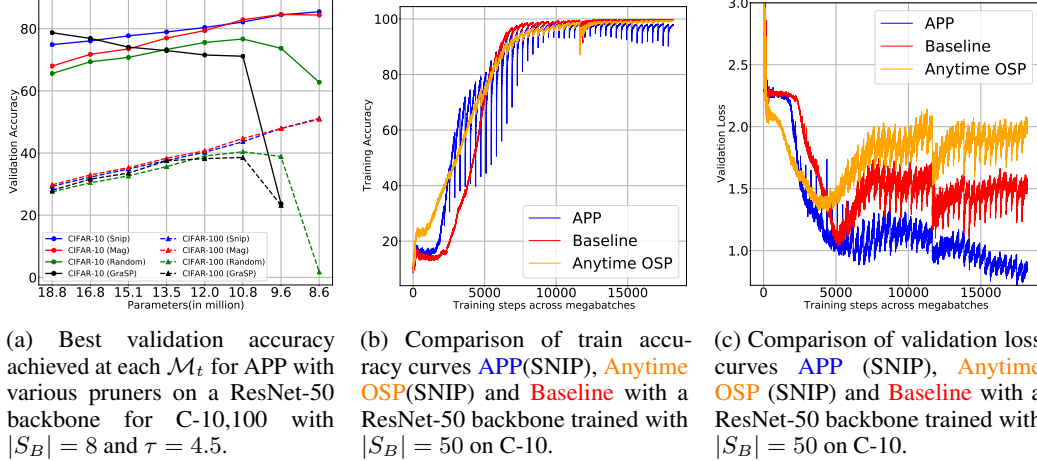


Figure 7: Change in CER during training of APP (SNIP), Anytime OSP (SNIP) and Baseline using a ResNet-50 on C-10 with varying number of megabatches ( $|S_B|$ ). X-axis represents the number of megabatches in the entire stream  $S_B$ .

Second, we also observe in Fig. 6c, that the validation loss curve for APP has a negative slope while approaching the completion of training over the complete stream  $S_B$ , while the curves for Anytime OSP and baseline models are significantly higher and plateauing, indicating saturation in learning capacity.

Furthermore, we also visualize the best validation accuracy achieved for APP with various pruners on a ResNet-50 backbone for C-10,100 with  $|S_B| = 8$  and  $\tau = 4.5$ . We observe that SNIP and magnitude-based pruning provide consistent and stable performance improvements over each megabatch in the stream  $S_B$ , while random pruning and GraSP cause instability and drop performance by a significant margin during training on the final megabatches in the stream  $S_B$ . Thus, we set SNIP to be the pruner of choice for APP by default for all of our experiments.

Finally, we visualize the change in CER during training for APP (SNIP), Anytime OSP (SNIP) and baseline using a ResNet-50 on C-10 by varying the total number of megabatches ( $|S_B|$ ) in the stream  $S_B$ . As shown in Fig. 7, APP (SNIP) consistently maintains a lower CER compared to its Anytime OSP and baseline counterparts under the short ( $|S_B| = 8$ ), moderate ( $|S_B| = 25$ ) and long ( $|S_B| = 50$ ) ALMA sequence.

#### 4.1.6 Restricted ImageNet full ALMA

Finally, we also conducted an experiment on the full restricted ImageNet Balanced dataset (32 x 32 downsampled version) using  $|S_B| = 3$  megabatches with each megabatch containing  $\mathcal{M}_t = 29839$  samples on a ResNet-50 trained using SGD and cyclic multidecay learning rate policy at each megabatch  $\mathcal{M}_t$ . As reported in Table 7, we observe that both APP and Anytime OSP models cause a drop in test accuracy and an increase in CER compared to the baseline model. However, APP reduces

the generalization gap by a margin of 1.845% for  $|S_B| = 3$  and 6.077% for  $|S_B| = 53$  compared to the baseline.

Table 7: Results on Restricted ImageNet (32 x 32) ALMA using SGD with cyclic multi-step decay at every  $\mathcal{M}_t$ .

Method	$ S_B $	$ \mathcal{M}_t $	Test Accuracy( $\uparrow$ )	CER( $\downarrow$ )	Generalization Gap( $\downarrow$ )
Baseline	3	29839	<b>86.318%</b>	<b>2046</b>	10.792%
Anytime OSP	-	-	84.55%(-1.768 %)	2384 (+338)	10.095%(-0.697 %)
APP	-	-	84.49%(-1.828 %)	2310 (+264)	<b>8.947%(-1.845 %)</b>
Baseline	53	1689	<b>86.782%</b>	<b>44702</b>	8.546%
Anytime OSP	-	-	86.492%(-0.29 %)	47431 (+2729)	7.179%(-1.367 %)
APP	-	-	83.333%(-3.449 %)	51728 (+7026)	<b>2.469%(-6.077 %)</b>

## 4.2 Transitions in generalization gap

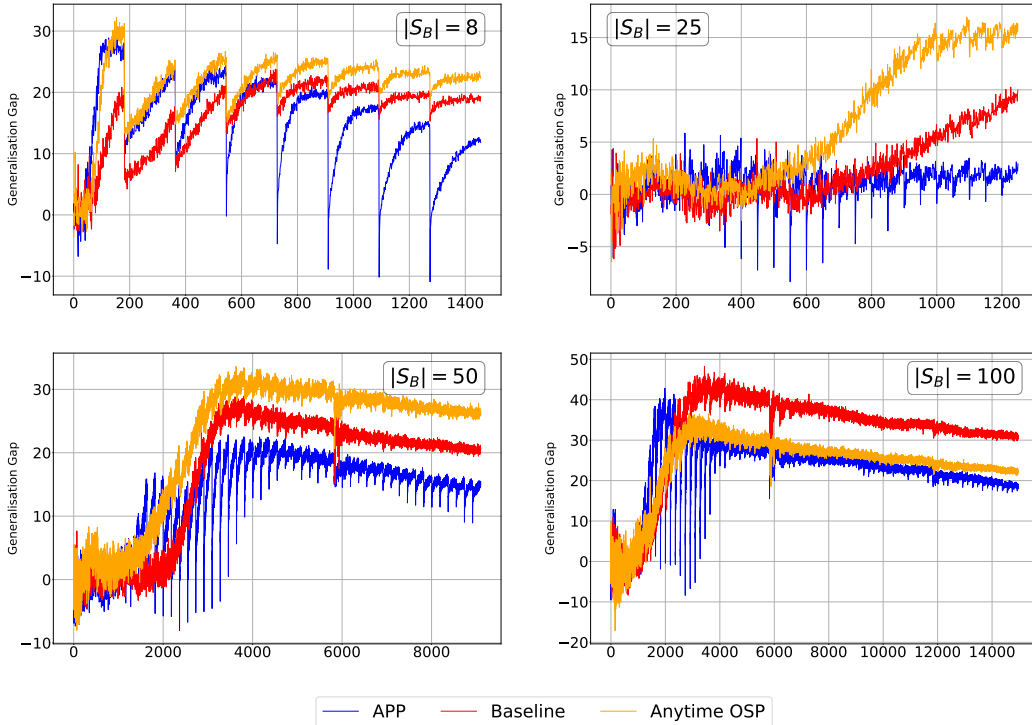


Figure 8: Generalization gap curves during training of APP (SNIP), Anytime OSP (SNIP) and Baseline using a ResNet-50 on C-10 with varying number of megabatches( $|S_B|$ ) with full replay. X-axis represents the total number of training iterations completed throughout the stream  $S_B$ .

While training the models for empirical validation, we observed a very interesting trend in the training dynamics, precisely the generalization gap, in the long-sequence ALMA. As defined in Section 3, the generalization gap is the difference observed between the training and validation accuracy across the complete training process over the stream  $S_B$ . The generalization gap is used to conclude whether a model is overfitting or underfitting, thus serving as an important criterion for the evaluation of models and investigating failure modes during model training. Similarly to the results reported in Nakkiran et al. [2021], we observe a non-monotonic transition in the generalization gap across APP, Anytime OSP, and baseline models during long-sequence ALMA training ( $|S_B| = (50, 100)$ ). In Fig. 8, we observe the generalization gap as a function of training iterations over the entire stream  $S_B$  for APP, Anytime OSP and baseline models using ResNet-50 backbone on C-10 with various

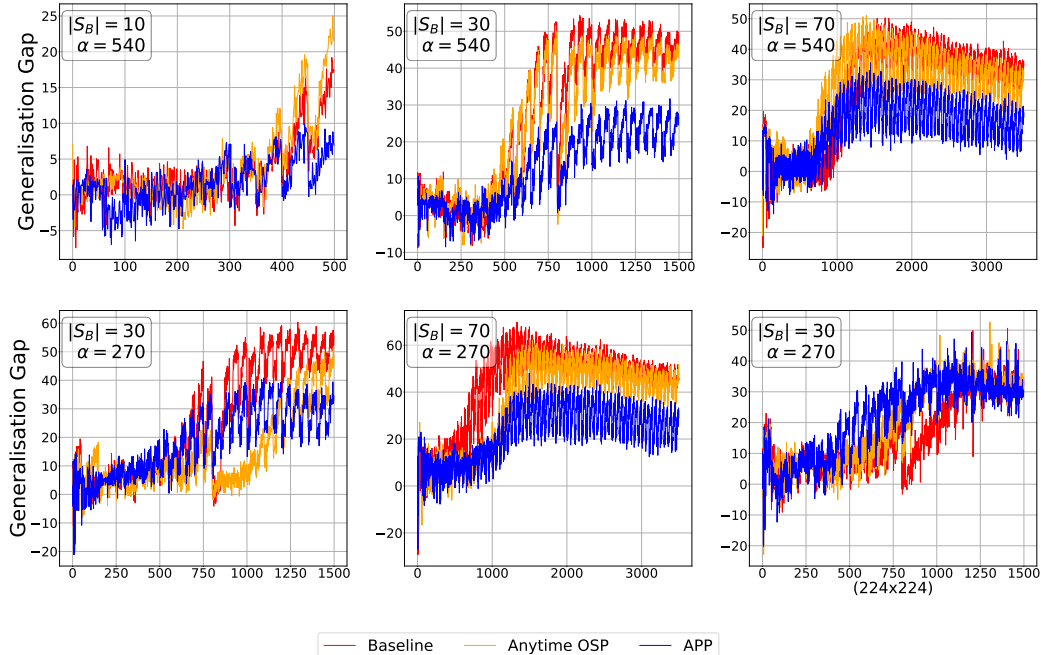


Figure 9: Generalization gap curves during training of APP (SNIP), Anytime OSP (SNIP) and Baseline for the experiments reported in Table 6.

number of megabatches ( $|S_B| = (8, 25, 50, 100)$ ). We observe in both  $|S_B| = 50$  and  $|S_B| = 100$ , a non-monotonic transition in the generalization gap where the model starts by underfitting, then sharply goes into the critical regime of overfitting, and subsequently has a gradual decrease in the generalization gap. We additionally observe that the generalization gap curve for APP tends to oscillate heavily in the critical regime, which might be attributed to pruning at the start of the megabatch under fewer data scenarios. Additionally, we also observe that for  $|S_B| = 25$ , the generalization gap for the Anytime OSP and the baseline model, rises sharply towards the end of training, while for APP it remains relatively stable.

We also visualize the generalization gap as a function of training iterations in Fig. 9 for the experiments reported in Table 6. As demonstrated in Fig. 8, we observe the same non-monotonic transition in the high number of megabatch  $|S_B| = 30, 70$  settings. In all subplots, it can be seen that APP consistently maintains a lower generalization gap compared to its Anytime OSP and baseline counterparts.

### 4.3 Layer-wise Pruning Distribution

In this section, we analyze the distribution of the pruned weights across the layers when using different pruners of choice for APP. In the experiment, we only visualize the difference between magnitude-based pruning and SNIP Lee et al. [2018], since random pruning and GraSP Wang et al. [2020b] lead to unstable training and therefore do not provide any meaningful insight. For the backbone, we used a ResNet-50 with an SGD + multidecay learning rate policy for the first megabatch  $\mathcal{M}_1$  only. Both models were trained with full replay for a total of  $|S_B| = 8$  megabatches, each megabatch  $\mathcal{M}_t$  having a total of  $|\mathcal{M}_t| = 6250$  samples.

As demonstrated in Fig. 10, we see that magnitude pruning leads to more weights of the initial layers being pruned at the initial megabatches compared to SNIP. Shang et al. [2016], Xiao et al. [2021] have demonstrated the importance of early convolution layers in the performance of deep convolution neural networks, and it is a well-accepted notion that early convolution layers are responsible for learning low-level features, such as edges, while later layers learn high-level features, such as texture. Since magnitude-based pruning removes a significant amount of early layer weights, this causes a drop in test accuracy compared to SNIP, which prunes more of the latter layers at the initial megabatches.

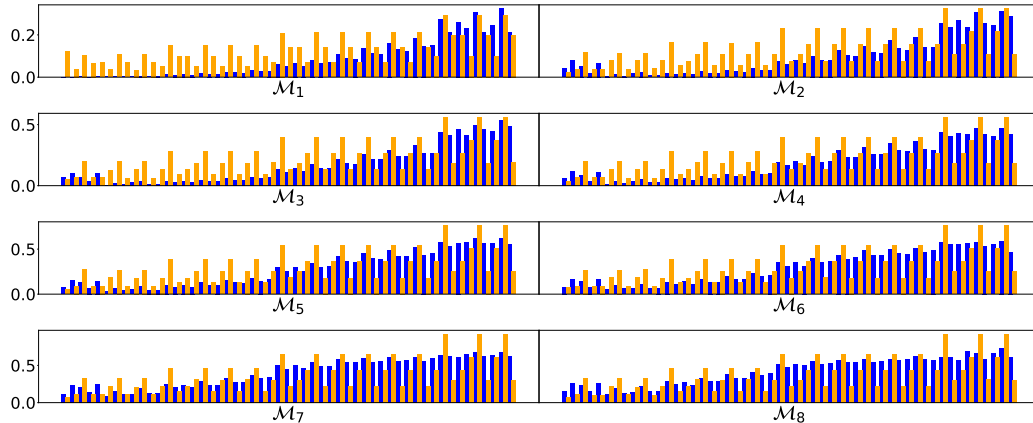


Figure 10: Progressive number of weights pruned at each megabatch  $\mathcal{M}_t$  for ALMA on ResNet-50 with APP for a total of  $|S_B| = 8$  megabatches on the CIFAR-10 dataset with full replay. For the experiment, we used the SGD + cyclic learning rate policy at only the first megabatch  $\mathcal{M}_1$ . **Blue** bars represent APP with SNIP as the pruner of choice while **Orange** bars represent APP with magnitude pruning. Both pruners were used for the same target sparsity  $\tau = 4.5$ . In each subplot, each bar corresponds to each layer of the network, and the  $y$ -axis represents the % of the weights pruned for that layer.

## 5 Reproducibility Statement

To ensure fair and reproducible experiments throughout our work, we enforced the following measures:

1. **Use of publicly available open source datasets:** As defined in subsection 4, throughout our research, we do empirical evaluation only using publicly available datasets - (a) CIFAR-10 Krizhevsky et al. [2009], (b) CIFAR-100 Krizhevsky et al. [2009], and (c) Restricted ImageNet Tsipras et al. [2018]. In our code, we also provide predefined dataloaders and augmentations that were used to construct the megabatches  $\mathcal{M}_t$ . None of the datasets used in this work contain sensitive or private information pertaining to an individual or a single entity against their consent.
2. **Use of open source frameworks and packages:** For all empirical experiments, we rely on packages and libraries that are accessible and available to the general public.

### 5.1 Hardware resources

For all experiments, we primarily used three different hardware configurations, as listed below:

1. 1 NVIDIA A100 GPU accelerator with 20 CPUs and 24 GB memory.
2. 1 NVIDIA V100 GPU accelerator with 20 CPUs and 18 GB memory.
3. 1 NVIDIA RTX 8000 GPU accelerator with 8,20 CPUs and 12 GB memory.

All CIFAR-10 and CIFAR-100 experiments were conducted using the NVIDIA RTX-8000 GPU, while the NVIDIA A100 and V100 were only used for restricted ImageNet experiments. Finally, we also used Google Colaboratory for initial proof-of-concept and ablation experiments.

## 6 Conclusion, Open Questions and Future Work

In this work, we introduced Anytime Progressive Pruning (APP), a novel way to progressively prune deep networks while training in an ALMA regime. We improvise on existing pruning at initialization strategies to design APP and perform an extensive empirical evaluation to validate performance improvement in various architectures and datasets. We found that pruning deep networks with APP while training in an ALMA setting causes a significant drop in the generalization gap compared to one-shot pruning methods and the dense baseline model.



We conclude this research with the remark that our work serves to lay the foundation for further exploration into dynamic and progressive pruning in sequential learning regimes. Although our work provides constructive insights into the training dynamics of progressive pruning, there are several questions that we hope can be subsequently explored based on this work, which are as follows.

1. How can we control the pruning rate at each megabatch  $\mathcal{M}_t$  without prior knowledge of the total number of megabatches in the stream  $S_B$ ?
2. What is the reason behind the non-monotonic transitions observed in the generalisation gap?
3. Although we hypothesize that the reason behind the oscillation (drop in test accuracy at the initial iteration of each megabatch) for APP is due to the regularization effect induced due to pruning, how can we formally prove this phenomenon?
4. Why does APP not work under no replay settings, while Anytime OSP does?

In addition to the above questions, in future work, we aim to further improve the performance of APP in no-replay settings by designing an optimal framework for data-constrained progressive pruning. We also aim to improve the performance of APP for greater target sparsity  $\tau$  and simultaneously perform a hyperparameter search to find the optimal hyperparameters for progressive pruning using APP. Finally, we also aim to transfer the progressive pruning setting to other tasks such as object detection and semantic segmentation.

## 7 Acknowledgements

The authors express their sincere gratitude to Gintare Karolina Dziugaite (Google Brain) and Himanshu Arora (Workday) for providing valuable initial feedback in refining the idea, and to Ajay Arasanipalai (UIUC) for helping with code review and ablation experiments.

## References

- Rahaf Aljundi, Punarjay Chakravarty, and Tinne Tuytelaars. Expert gate: Lifelong learning with a network of experts. In *Proceedings of the IEEE Conference on Computer Vision and Pattern Recognition*, pages 3366–3375, 2017.
- Yoram Baram, Ran El Yaniv, and Kobi Luz. Online choice of active learning algorithms. *Journal of Machine Learning Research*, 5(Mar):255–291, 2004.
- Eden Belouadah and Adrian Popescu. Deesil: Deep-shallow incremental learning. In *Proceedings of the European Conference on Computer Vision (ECCV)*, pages 0–0, 2018.
- Eden Belouadah and Adrian Popescu. Il2m: Class incremental learning with dual memory. In *The IEEE International Conference on Computer Vision (ICCV)*, October 2019.
- Eden Belouadah and Adrian Popescu. Scail: Classifier weights scaling for class incremental learning, 2020.
- Shai Ben-David, Eyal Kushilevitz, and Yishay Mansour. Online learning versus offline learning. *Machine Learning*, 29(1):45–63, 1997.
- Melanie Bernhardt, Daniel C Castro, Ryutaro Tanno, Anton Schwaighofer, Kerem C Tezcan, Miguel Monteiro, Shruthi Bannur, Matthew Lungren, Aditya Nori, Ben Glocker, et al. Active label cleaning: improving dataset quality under resource constraints. *arXiv preprint arXiv:2109.00574*, 2021.
- Davis Blalock, Jose Javier Gonzalez Ortiz, Jonathan Frankle, and John Guttag. What is the state of neural network pruning? *Proceedings of machine learning and systems*, 2:129–146, 2020.
- Léon Bottou et al. Online learning and stochastic approximations. *On-line learning in neural networks*, 17(9):142, 1998.
- Mateusz Buda, Atsuto Maki, and Maciej A Mazurowski. A systematic study of the class imbalance problem in convolutional neural networks. *Neural Networks*, 106:249–259, 2018.
- Lucas Caccia, Jing Xu, Myle Ott, Marc’ Aurelio Ranzato, and Ludovic Denoyer. On anytime learning at macroscale. *arXiv preprint arXiv:2106.09563*, 2021.
- Francisco M Castro, Manuel J Marín-Jiménez, Nicolás Guil, Cordelia Schmid, and Karteek Alahari. End-to-end incremental learning. In *Proceedings of the European Conference on Computer Vision (ECCV)*, pages 233–248, 2018.
- Tianlong Chen, Zhenyu Zhang, Sijia Liu, Shiyu Chang, and Zhangyang Wang. Long live the lottery: The existence of winning tickets in lifelong learning. In *International Conference on Learning Representations*, 2020.
- Tianlong Chen, Zhenyu Zhang, Sijia Liu, Shiyu Chang, and Zhangyang Wang. Long live the lottery: The existence of winning tickets in lifelong learning. In *International Conference on Learning Representations*, 2021. URL <https://openreview.net/forum?id=LXMSvPmsm0g>.
- Christos Dimitrakakis and Christian Savu-Krohn. Cost-minimising strategies for data labelling: optimal stopping and active learning. In *International Symposium on Foundations of Information and Knowledge Systems*, pages 96–111. Springer, 2008.
- Logan Engstrom, Andrew Ilyas, Hadi Salman, Shibani Santurkar, and Dimitris Tsipras. Robustness (python library), 2019. URL <https://github.com/MadryLab/robustness>.
- Jonathan Frankle and Michael Carbin. The lottery ticket hypothesis: Finding sparse, trainable neural networks. *arXiv preprint arXiv:1803.03635*, 2018.
- Jonathan Frankle, Gintare Karolina Dziugaite, and M Daniel. Roy, and michael carbin. the lottery ticket hypothesis at scale. *arXiv preprint arXiv:1903.01611*, 2(3), 2019a.
- Jonathan Frankle, Gintare Karolina Dziugaite, Daniel M Roy, and Michael Carbin. Stabilizing the lottery ticket hypothesis. *arXiv preprint arXiv:1903.01611*, 2019b.

- Siavash Golkar, Michael Kagan, and Kyunghyun Cho. Continual learning via neural pruning. *arXiv preprint arXiv:1903.04476*, 2019.
- John J Grefenstette and Connie Loggia Ramsey. An approach to anytime learning. In *Machine Learning Proceedings 1992*, pages 189–195. Elsevier, 1992.
- Song Han, Huizi Mao, and William J Dally. Deep compression: Compressing deep neural networks with pruning, trained quantization and huffman coding. *arXiv preprint arXiv:1510.00149*, 2015a.
- Song Han, Jeff Pool, John Tran, and William Dally. Learning both weights and connections for efficient neural network. In *Advances in neural information processing systems*, pages 1135–1143, 2015b.
- Chen He, Ruiping Wang, Shiguang Shan, and Xilin Chen. Exemplar-supported generative reproduction for class incremental learning. In *British Machine Vision Conference*, 2018.
- Haibo He and Eduardo A Garcia. Learning from imbalanced data. *IEEE Transactions on knowledge and data engineering*, 21(9):1263–1284, 2009.
- Kaiming He, Xiangyu Zhang, Shaoqing Ren, and Jian Sun. Deep residual learning for image recognition. In *Proceedings of the IEEE conference on computer vision and pattern recognition*, pages 770–778, 2016.
- Yihui He, Xiangyu Zhang, and Jian Sun. Channel pruning for accelerating very deep neural networks. In *Proceedings of the IEEE International Conference on Computer Vision*, pages 1389–1397, 2017.
- Khurram Javed and Faisal Shafait. Revisiting distillation and incremental classifier learning. In *Asian Conference on Computer Vision*, pages 3–17. Springer, 2018.
- Ronald Kemker and Christopher Kanan. Fearnnet: Brain-inspired model for incremental learning. *arXiv preprint arXiv:1711.10563*, 2017.
- Alex Krizhevsky, Geoffrey Hinton, et al. Learning multiple layers of features from tiny images. 2009.
- Yann LeCun, John S Denker, and Sara A Solla. Optimal brain damage. In *Advances in neural information processing systems*, pages 598–605, 1990.
- Namhoon Lee, Thalaisyasingam Ajanthan, and Philip HS Torr. Snip: Single-shot network pruning based on connection sensitivity. *arXiv preprint arXiv:1810.02340*, 2018.
- Namhoon Lee, Thalaisyasingam Ajanthan, and Philip H. S. Torr. Snip: Single-shot network pruning based on connection sensitivity, 2019.
- Zhizhong Li and Derek Hoiem. Learning without forgetting. *IEEE transactions on pattern analysis and machine intelligence*, 40(12):2935–2947, 2017.
- Zhuang Liu, Jianguo Li, Zhiqiang Shen, Gao Huang, Shoumeng Yan, and Changshui Zhang. Learning efficient convolutional networks through network slimming. In *Proceedings of the IEEE international conference on computer vision*, pages 2736–2744, 2017.
- Zhuoming Liu, Hao Ding, Huaping Zhong, Weijia Li, Jifeng Dai, and Conghui He. Influence selection for active learning. In *Proceedings of the IEEE/CVF International Conference on Computer Vision (ICCV)*, pages 9274–9283, October 2021.
- Jian-Hao Luo, Jianxin Wu, and Weiyao Lin. Thinet: A filter level pruning method for deep neural network compression. In *Proceedings of the IEEE international conference on computer vision*, pages 5058–5066, 2017.
- Eran Malach, Gilad Yehudai, Shai Shalev-Schwartz, and Ohad Shamir. Proving the lottery ticket hypothesis: Pruning is all you need. In *International Conference on Machine Learning*, pages 6682–6691. PMLR, 2020.
- Arun Mallya, Dillon Davis, and Svetlana Lazebnik. Piggyback: Adapting a single network to multiple tasks by learning to mask weights. In *Proceedings of the European Conference on Computer Vision (ECCV)*, pages 67–82, 2018.

- Pavlo Molchanov, Arun Mallya, Stephen Tyree, Iuri Frosio, and Jan Kautz. Importance estimation for neural network pruning. In *Proceedings of the IEEE Conference on Computer Vision and Pattern Recognition*, pages 11264–11272, 2019.
- Preetum Nakkiran, Gal Kaplun, Yamini Bansal, Tristan Yang, Boaz Barak, and Ilya Sutskever. Deep double descent: Where bigger models and more data hurt. *Journal of Statistical Mechanics: Theory and Experiment*, 2021(12):124003, 2021.
- Fredrik Olsson. A literature survey of active machine learning in the context of natural language processing. 2009.
- Sinno Jialin Pan and Qiang Yang. A survey on transfer learning. *IEEE Transactions on knowledge and data engineering*, 22(10):1345–1359, 2009.
- Connie Loggia Ramsey and John J Grefenstette. Case-based anytime learning. In *Case Based Reasoning: Papers from the 1994 Workshop*, pages 91–95. AAAI Press Menlo Park, California, 1994.
- Sylvestre-Alvise Rebuffi, Alexander Kolesnikov, Georg Sperl, and Christoph H Lampert. icarl: Incremental classifier and representation learning. In *Proceedings of the IEEE conference on Computer Vision and Pattern Recognition*, pages 2001–2010, 2017.
- Sylvestre-Alvise Rebuffi, Hakan Bilen, and Andrea Vedaldi. Efficient parametrization of multi-domain deep neural networks. In *Proceedings of the IEEE Conference on Computer Vision and Pattern Recognition*, pages 8119–8127, 2018.
- Mark B Ring. Child: A first step towards continual learning. In *Learning to learn*, pages 261–292. Springer, 1998.
- Mark Bishop Ring et al. Continual learning in reinforcement environments. 1994.
- Amir Rosenfeld and John K Tsotsos. Incremental learning through deep adaptation. *IEEE transactions on pattern analysis and machine intelligence*, 2018.
- Olga Russakovsky, Jia Deng, Hao Su, Jonathan Krause, Sanjeev Satheesh, Sean Ma, Zhiheng Huang, Andrej Karpathy, Aditya Khosla, Michael Bernstein, et al. Imagenet large scale visual recognition challenge. *International journal of computer vision*, 115(3):211–252, 2015.
- Andrei A Rusu, Neil C Rabinowitz, Guillaume Desjardins, Hubert Soyer, James Kirkpatrick, Koray Kavukcuoglu, Razvan Pascanu, and Raia Hadsell. Progressive neural networks. *arXiv preprint arXiv:1606.04671*, 2016.
- David Saad. Online algorithms and stochastic approximations. *Online Learning*, 5:6–3, 1998.
- Doyen Sahoo, Quang Pham, Jing Lu, and Steven CH Hoi. Online deep learning: Learning deep neural networks on the fly. *arXiv preprint arXiv:1711.03705*, 2017.
- Burr Settles. Active learning literature survey. 2009.
- Burr Settles, Mark Craven, and Lewis Friedland. Active learning with real annotation costs. In *Proceedings of the NIPS workshop on cost-sensitive learning*, volume 1. Vancouver, CA:, 2008.
- Wenling Shang, Kihyuk Sohn, Diogo Almeida, and Honglak Lee. Understanding and improving convolutional neural networks via concatenated rectified linear units. In *international conference on machine learning*, pages 2217–2225. PMLR, 2016.
- Karen Simonyan and Andrew Zisserman. Very deep convolutional networks for large-scale image recognition. *arXiv preprint arXiv:1409.1556*, 2014.
- Ghada Sokar, Decebal Constantin Mocanu, and Mykola Pechenizkiy. Spacenet: Make free space for continual learning. *arXiv preprint arXiv:2007.07617*, 2020.
- Hidenori Tanaka, Daniel Kunin, Daniel LK Yamins, and Surya Ganguli. Pruning neural networks without any data by iteratively conserving synaptic flow. *arXiv preprint arXiv:2006.05467*, 2020.

- Sebastian Thrun. A lifelong learning perspective for mobile robot control. In *Intelligent robots and systems*, pages 201–214. Elsevier, 1995.
- Sebastian Thrun. Lifelong learning algorithms. In *Learning to learn*, pages 181–209. Springer, 1998.
- Dimitris Tsipras, Shibani Santurkar, Logan Engstrom, Alexander Turner, and Aleksander Madry. Robustness may be at odds with accuracy. *arXiv preprint arXiv:1805.12152*, 2018.
- Gido M Van de Ven and Andreas S Tolias. Three scenarios for continual learning. *arXiv preprint arXiv:1904.07734*, 2019.
- Chaoqi Wang, ChaoQi Wang, Guodong Zhang, and Roger B. Grosse. Picking winning tickets before training by preserving gradient flow. *ArXiv*, abs/2002.07376, 2020a.
- Chaoqi Wang, Guodong Zhang, and Roger Grosse. Picking winning tickets before training by preserving gradient flow. *arXiv preprint arXiv:2002.07376*, 2020b.
- Huan Wang, Can Qin, Yulun Zhang, and Yun Fu. Emerging paradigms of neural network pruning. *arXiv preprint arXiv:2103.06460*, 2021.
- Yu-Xiong Wang, Deva Ramanan, and Martial Hebert. Growing a brain: Fine-tuning by increasing model capacity. In *Proceedings of the IEEE Conference on Computer Vision and Pattern Recognition*, pages 2471–2480, 2017.
- Tete Xiao, Piotr Dollar, Mannat Singh, Eric Mintun, Trevor Darrell, and Ross Girshick. Early convolutions help transformers see better. *Advances in Neural Information Processing Systems*, 34, 2021.
- Sergey Zagoruyko and Nikos Komodakis. Wide residual networks. *arXiv preprint arXiv:1605.07146*, 2016.
- Tianyun Zhang, Kaiqi Zhang, Shaokai Ye, Jian Tang, Wujie Wen, Xue Lin, Makan Fardad, and Yanzhi Wang. Adam-admm: A unified, systematic framework of structured weight pruning for dnns. *arXiv preprint arXiv:1807.11091*, 2018.
- Hao Zhou, Jose M Alvarez, and Fatih Porikli. Less is more: Towards compact cnns. In *European Conference on Computer Vision*, pages 662–677. Springer, 2016.